



**Fermi National Accelerator Laboratory**

**FERMILAB-Conf-98/194-E**

**E892**

## **The CMS Central Hadron Calorimeter: Update**

J. Freeman

For the E892 Collaboration

*Fermi National Accelerator Laboratory  
P.O. Box 500, Batavia, Illinois 60510*

June 1998

Presented at the *Workshop on Scintillator and Fiber Detectors, (SCIFI97)*,  
Notre Dame, Indiana, October 3-6, 1997

## **Disclaimer**

*This report was prepared as an account of work sponsored by an agency of the United States Government. Neither the United States Government nor any agency thereof, nor any of their employees, makes any warranty, expressed or implied, or assumes any legal liability or responsibility for the accuracy, completeness, or usefulness of any information, apparatus, product, or process disclosed, or represents that its use would not infringe privately owned rights. Reference herein to any specific commercial product, process, or service by trade name, trademark, manufacturer, or otherwise, does not necessarily constitute or imply its endorsement, recommendation, or favoring by the United States Government or any agency thereof. The views and opinions of authors expressed herein do not necessarily state or reflect those of the United States Government or any agency thereof.*

## **Distribution**

*Approved for public release; further dissemination unlimited.*

# The CMS Central Hadron Calorimeter: Update

Jim Freeman

*Fermi National Accelerator Laboratory, Batavia, Illinois 60510  
Representing the CMS Hadron Calorimeter Group*

**Abstract.** The CMS central hadron calorimeter is a brass absorber/ scintillator sampling structure. We describe details of the mechanical and optical structure. We also discuss calibration techniques, and finally the anticipated construction schedule.

## OVERVIEW

The CMS detector is a general purpose experiment that will operate at the Large Hadron Collider at CERN. The heart of the CMS detector is a large volume 4T superconducting solenoid. The solenoid is 13 meters long with an inner radius of 3 meters. Inside the solenoid are tracking detectors, followed by an electromagnetic calorimeter (ECAL) made of lead tungstate crystals and finally the hadron calorimeter (HCAL). Figure 1 shows a quarter section of the CMS detector design.

A major function of the HCAL is the measurement of missing transverse energy. For this measurement, Gaussian resolution is not as important as elimination of low energy tails in the response function. With this in mind, the CMS HCAL design strives to eliminate dead material that causes energy loss, and to maximize the calorimeter thickness. The location of the HCAL inside the magnetic field requires that the calorimeter be non-magnetic. The absorber chosen is “cartridge brass”, 70% brass and 30% zinc.

The central HCAL covers the  $\eta$  range of  $-3 < \eta < 3$  and  $0 < \phi < 2\pi$ . The central HCAL is physically composed of 2 regions, the barrel ( $|\eta| < 1$ ), and the endcap, which extends to  $|\eta| = 3$ . The very forward region of CMS,  $3 < |\eta| < 5$ , is covered by a quartz fiber calorimeter, and is discussed elsewhere in these proceedings.<sup>1</sup> The tower granularity is chosen to be  $\delta(\eta)$  times  $\delta(\phi) = 0.87 \times 0.87$ . The segmentation is commensurate with the granularity of ECAL, and is also sufficient for jet reconstruction.<sup>2</sup> Properties of the HCAL are shown in Table 1.

The active medium of the calorimeter is scintillator plastic, read out with wavelength shifting (WLS) optical fibers. This technique uses scintillator tiles to sample the shower. Wave-shifting fiber imbedded in the tile traps the scintillator light and clear fiber spliced to the WLS fiber carries the light to photo-transducers. The technique has been refined and applied to the CDF endcap upgrade calorimeter at

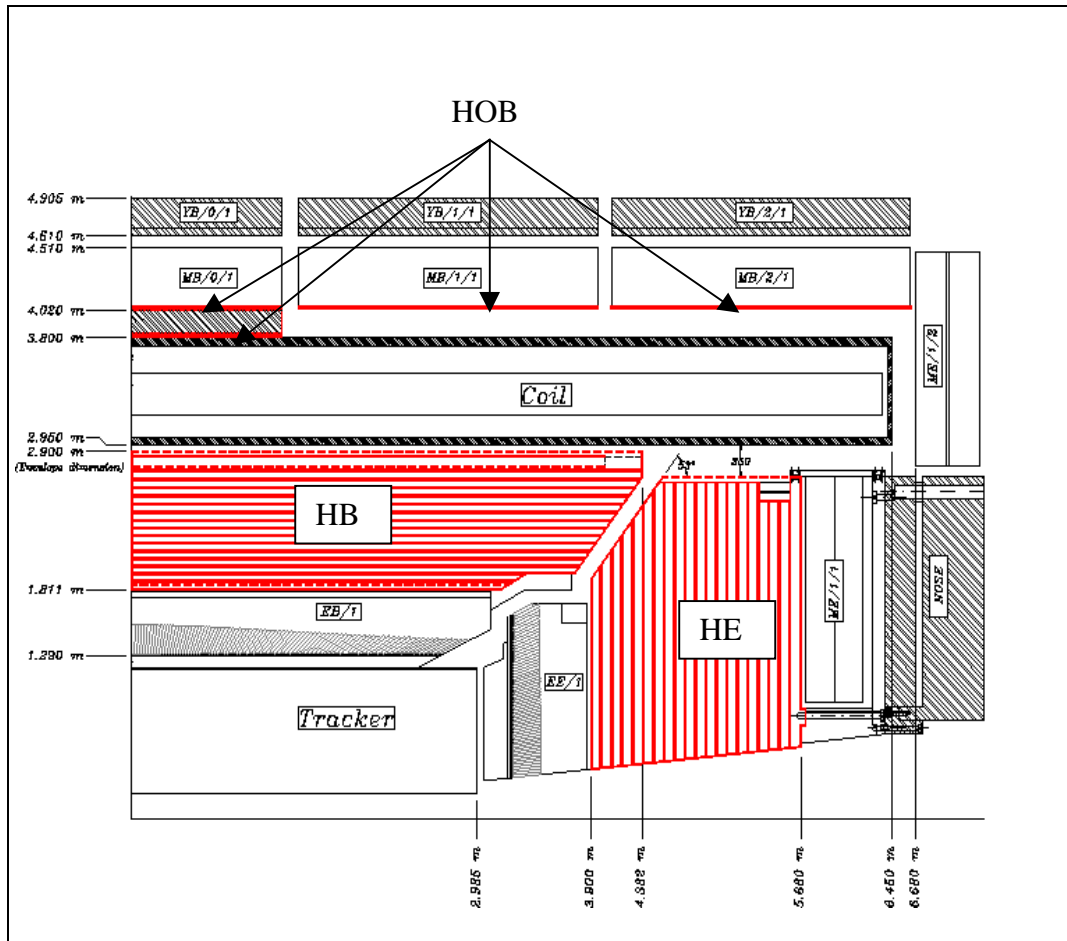


Figure 1. Quarter section of the CMS central detector.

Fermilab.<sup>3,4,5</sup> With this technique, the samples are thin. They require only 0.9 cm of thickness between absorber plates, so a high-density calorimeter is maintained.

The choice of scintillator for readout provides a calorimeter that is fast, stable and reliable, and radiation-resistant. More than 90% of the scintillation light will be collected within a 50 ns time window. The radiation dose for the scintillators at the high  $\eta$  end of the endcap calorimeter is large, 2 to 4 Mrads for the life of the experiment. This dose will damage the scintillators. We use a strategy of multiple longitudinal samples of the calorimeter in this region. By recalibrating the relative weights of the multiple samples on a yearly basis, we will be able to minimize the effect of radiation damage on the calorimeter resolution constant term.<sup>6</sup>

Figure 2 shows the mechanical structure of a wedge of the central HCAL barrel. The barrel HCAL is made of  $\delta(\phi) = 20^\circ$  wedges. Each wedge extends from  $\eta = 0$  to the high  $\eta$  boundary,  $\eta \cong 1$ . A wedge is about 4.5 meters long, and installed in CMS will extend from an inner radius of 1.8 meters to 2.9 meters. Each wedge weighs

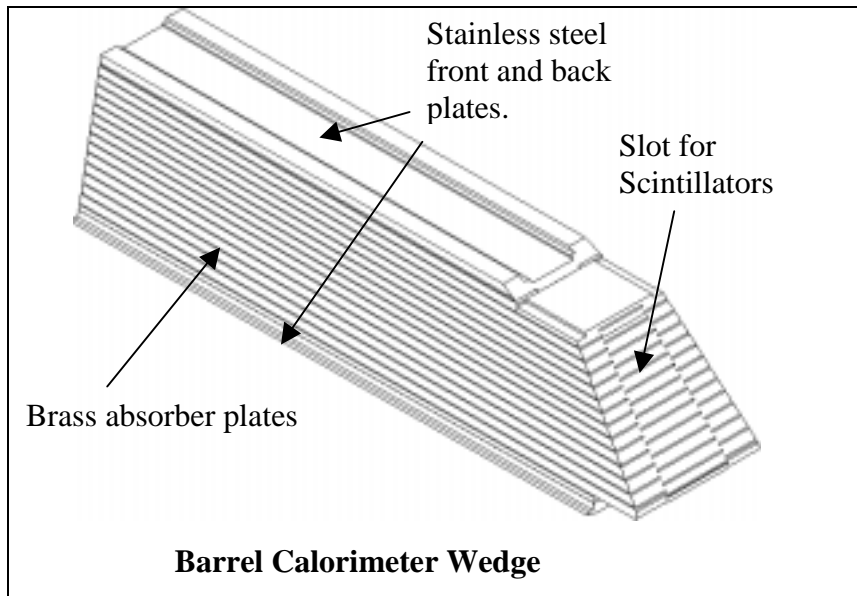


Figure 2. Isometric view of HCAL wedge showing front and back stainless steel plates, interior brass absorber plates, and slots for scintillator trays.

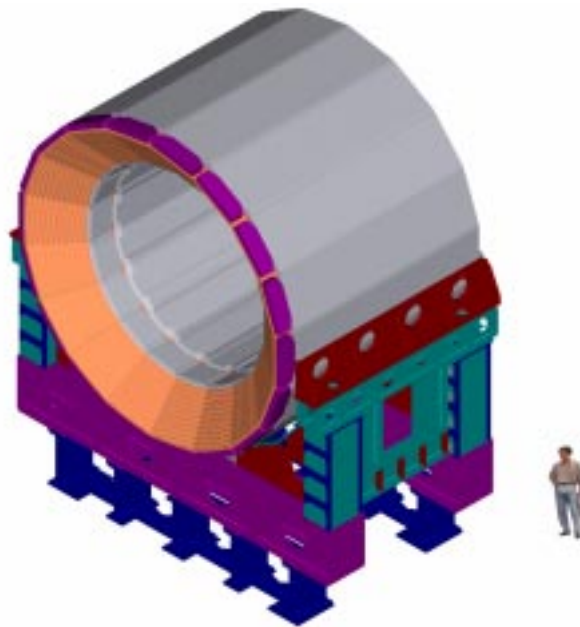


Figure 3. A half barrel of the hadron calorimeter resting on its installation cradle.

about 30 metric tons. A wedge is composed of 6 cm thick inner and outer stainless steel plates (for mechanical strength), with 6 cm thick brass absorber samples inside.

The entire internal structure is bolted together using about 2000 bolts. A set of 18 wedges are then bolted together to form a half-barrel ring, weighing about 500 metric tons. There are two such rings, one of which is shown in Figure 3.

The absorber structure is designed with alternating "staggered" slots for the scintillators. Thus the (4 tower wide in phi) wedge starts with a slot to accommodate scintillators for the middle 2 towers, then 1/2 of an absorber sample later in depth, have separate slots for the outer 2 towers. The staggering of the absorber plates provides a rigid mechanical structure, with no projective dead regions. Each slot runs the full length (in  $\eta$ ) of the wedge. Long thin scintillator "tile trays" will be inserted from the high  $\eta$  end, and optical cables will carry the scintillation light to the photodetectors.

Tight mechanical tolerances on the plates (and lack of distortion because of bolting) allows the design to have  $\leq 2$  mm of air gap between adjacent wedges. In addition, only a 9.5 mm high slot is needed to accommodate the 7.5 mm thick scintillator packages.

The construction of the endcap hadron calorimeter is logically similar to the barrel. Each endcap is a monolithic structure, bolted together from "pizza slice" shaped plates of brass. Again the plates are staggered to provide alternating slots for the scintillator tile trays. The endcap HCAL has 8 cm thick brass sampling.

Figure 4 shows the total number of interaction lengths of material provided by the ECAL (1.0  $\lambda$ ) and the HCAL. We see that at  $\eta=0$ , the combined calorimeter is somewhat thin,  $\approx 7.0 \lambda$ . Therefore our design places an additional scintillator sample outside the solenoid, the Outer HCAL Barrel (HOB). Figure 4 also shows the resulting total number of interaction lengths in the calorimeter. The placement of HOB is shown in Figure 1.

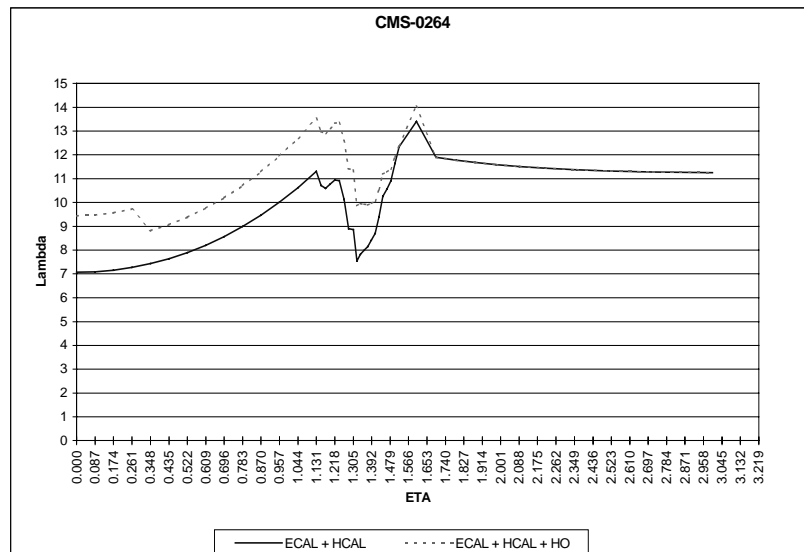


Figure 4. Interaction lengths vs eta for the ECAL +HCAL, and for the ECAL + HCAL +Outer Calorimeter.

## OPTICAL SYSTEM

The CMS HCAL optical system contains of approximately 70,000 individual scintillator tiles. Since the optical systems for the barrel and endcap HCAL are very similar, we will concentrate on the description of the barrel. The optical system is illustrated in Figure 5. Scintillation light from the scintillator tiles is captured in an embedded WLS fiber. The WLS fiber is mirrored on one end with an aluminum sputtered coating. The other end of the fiber is thermally welded to a clear fiber that carries the light to the high eta edge of the tile tray, terminating in an optical connector. An optical cable attached to the connector carries the light to the readout box at the outer radius of the HCAL wedge. Finally, the light from all tiles in a tower readout segment are ganged together and illuminate a pixel of a multi-pixel hybrid photodiode (HPD), the optical transducer used in the central HCAL.

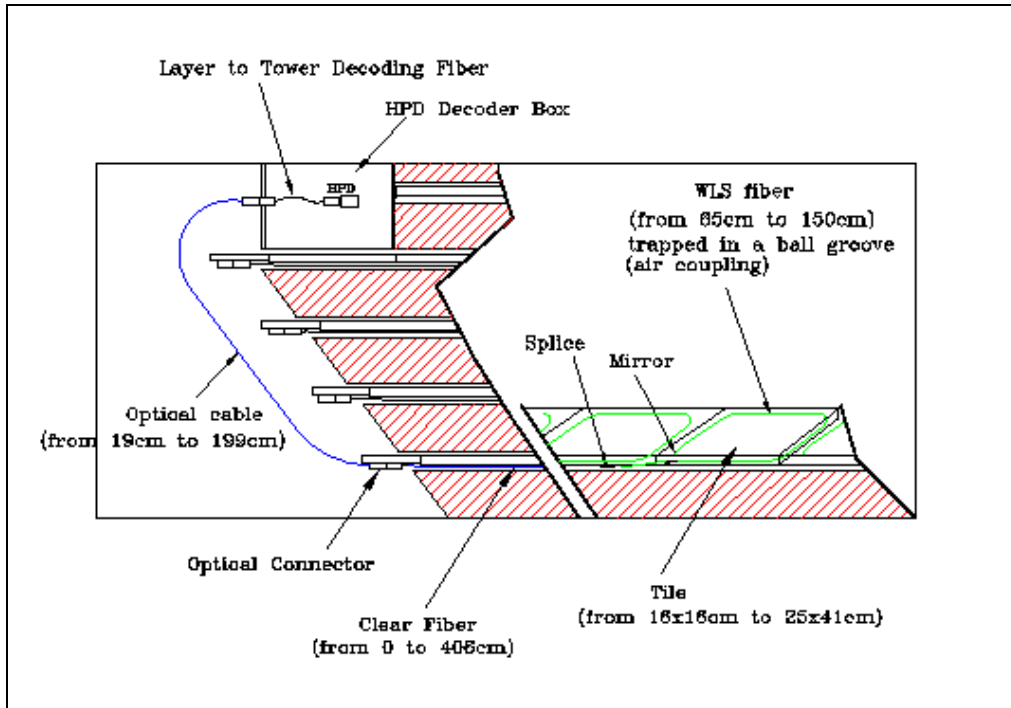


Figure 5. The layout of the optical readout of the HCAL.

The scintillators are organized into tile trays, as shown in Figure 6 for the barrel calorimeter. The trays are either 1 or 2 tiles wide in  $\phi$  to match the slots shown in Figure 2, and the full length of the barrel (16 tiles) in  $\eta$ .

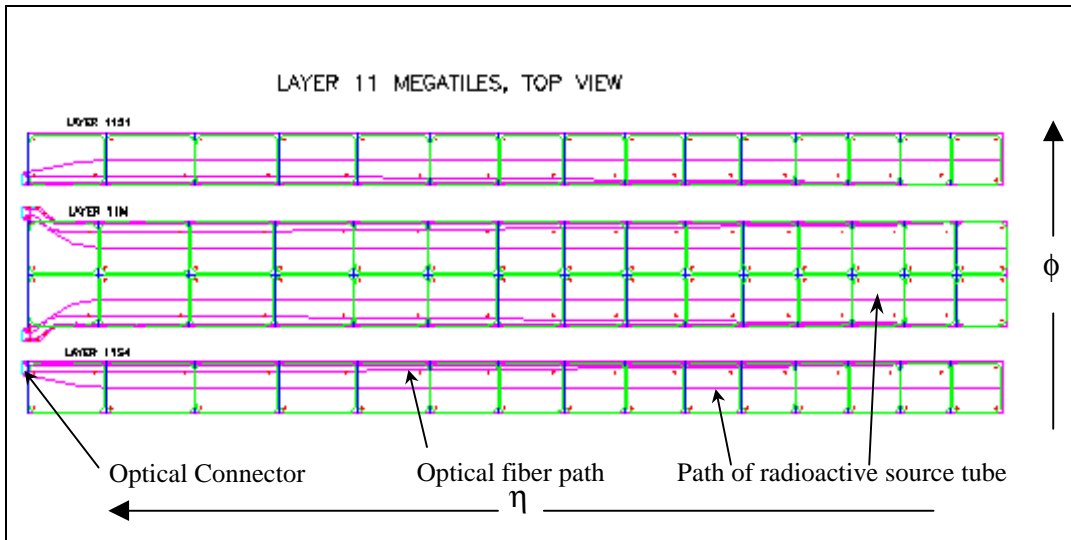


Figure 6. Scintillator tile trays to be inserted in the high-eta end of the wedge absorber.

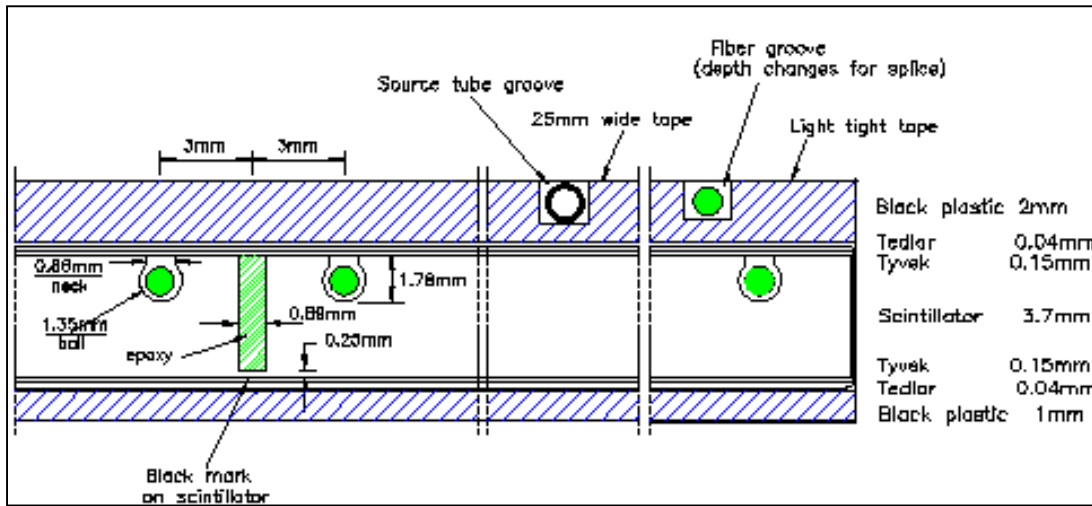


Figure 7. A cross section of the scintillator tile tray.

The cross section of the tile tray is shown in Figure 7. The 3.7 mm thick scintillator tiles are covered with white reflective Tyvek plastic, wrapped in opaque Tedlar black film, and then sandwiched between top and bottom cover plates. The entire package is connected together by small through-bolts. The thin bottom cover plate provides mechanical protection. The 2 mm thick top plate protects the tiles and supplies a path for the fibers from the tiles to travel to the high  $|\eta|$  end of the tile tray. There, the fibers are terminated into multi-fiber optical connectors. Optical cables carry the light onward to photodetector decoder boxes where the light from each tile is

organized into readout towers. Our baseline choices for optical materials are Kuraray SCSN81 for the scintillator, Kuraray multi-clad Y-11 (K-27 fluor) for the wave-shifting fiber, and Kuraray multi-clad clear fiber. With these materials, typical light-yields are about 2 photoelectrons per minimum-ionizing particle per scintillator layer.

## CALIBRATION

Quality control and calibration schemes are built into the optical system from the beginning. After assembly of the tile trays, a collimated  $\text{Cs}^{137}$  source is used to test the tiles. By measuring the induced radioactive source current after a photodetector, the collimated source measurement establishes the absolute response of the tiles. At the same time a moving wire source is used for cross calibration. Figure 6 shows the 2 mm top cover plate carrying "source tubes". The source tubes are stainless steel tubes that terminate into source-tube connectors that allow them to be "plumbed" to tubes from a moving wire source system.

In the moving wire source system, an approximate point source at the end of a wire moves through the source tubes to excite the scintillators. The source position relative to the tile is well controlled by the permanently attached source tube. Because of the fixed geometry of the source tube relative to the tile, the ratio of response of collimated to wire source is stable. The moving wire source ( $\text{Cs}^{137}$ ) is basically an isotropic source. The scintillator response changes by approximately 1% per 0.1 mm of separation between the scintillator and the source. Thus meaningful measurements with the wire source require that the stability of the placement of the wire source relative to scintillator must be controlled to order 0.1 mm. This is achieved by permanent attachment of the source tubes on the tile trays.

After the tile-trays have been installed into the absorber, the wire source is again used to test for system stability. Since the geometry of the wire source tube relative to the scintillator is unchanged, the measurement of wire-source response allows for reference back to the original QC test using the collimated source. A small number of the source tubes will be accessible during operation of CMS. These tubes will be periodically re-tested to verify stability.

A laser flasher system will also be used to directly excite the photodetectors. This system will be used on a periodic basis to track the gain of the photodetector/amplifier/digital readout system.

The stability of ratio of wire source measurement to collimated source measurement (i.e. to the true tile absolute response) provides a convenient way to carry test beam calibrations to the actual CMS detector. A subset of the barrel wedges will be extensively studied in test beam. Their calorimeter towers will have their pion response measured with test beams. In addition the wire-source system will measure the "fingerprint" of each tower's optical longitudinal response. An effective "pion-weighted source response" will be calculated by convoluting the measured longitudinal optical profile with an average pion longitudinal profile. Then the ratio of actual test beam response to pion-weighted source response will be used to carry test beam calibration to wedges in CMS that were not exposed to beams. From past experience on CDF, an initial absolute calibration of 2 - 3% is expected for wedges

that are not calibrated by the test beams.<sup>7</sup> This is small compared to the constant term of the HCAL resolution.

The initial absolute calibration can be improved by using in-situ physics calibrations while CMS is operating.<sup>8</sup> One likely signal is  $t\bar{t}$  production, where the top quarks then decay into  $W+b$ . One  $W$  is required to decay into jets, while the other is required to decay into lepton + neutrino to provide a trigger. For events that have 2 tagged  $b$ -jet's, CDF has shown that it can readily reconstruct the  $W$  boson that decays into jets. They measure a rms/mean of about 9 GeV / 81 GeV for 8 reconstructed top events in  $100 \text{ pb}^{-1}$  of data.

A similar analysis has been performed using a simulation of the CMS detector. There, even in the presence of the  $\sim 30$  minimum-bias events anticipated at the ultimate luminosity of  $10^{34}$ , the  $W$  into 2-jet decay can be reliably reconstructed. The results expected for one month of LHC running at  $10^{33}$  is shown in Figure 8. The LHC,  $t\bar{t}$  production will supply a ready source of di-jet events that reconstruct into a fixed mass and will help with calibration as well as understanding systematics of jet clustering. Other methods such as jet-jet and jet-gamma energy balance are also possible.

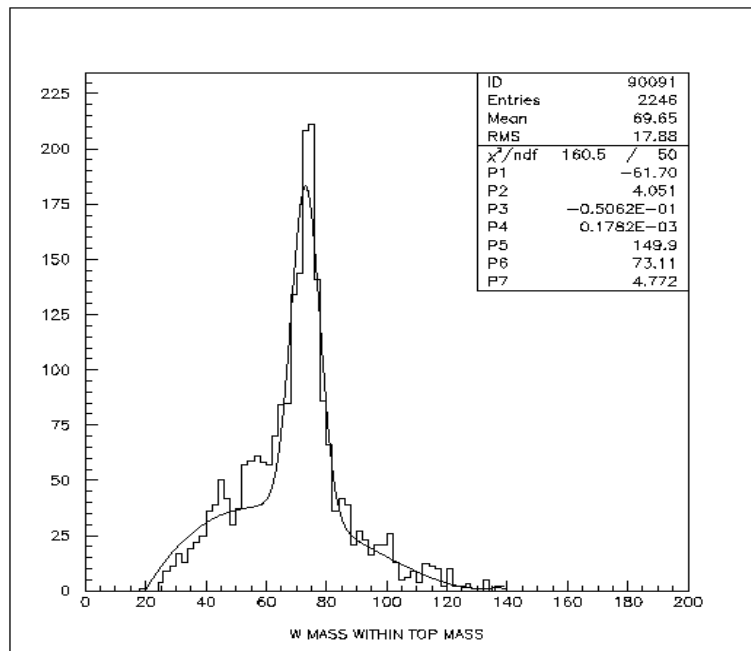


Figure 8. Reconstructed  $W$  decays into 2 quarks for double-tagged  $t\bar{t}$  events

## PHOTODETECTORS

The barrel photodetectors are positioned at the high  $|\eta|$  / large radius of the barrel HCAL, inside the 4T magnetic field. The corresponding location for photodetectors for the endcap calorimeter is at the large radius, large  $z$  corner. Because of the placement of the photodetectors, conventional photomultiplier tubes are unusable. Instead a recently developed transducer, the hybrid photodiode, HPD, has been adopted. The HPD is a proximity-focused device consisting of a vacuum envelop, a conventional photocathode, and a reverse-biased silicon diode. A high accelerating voltage (of order 10kV) is supplied between the photocathode and the silicon diode. Photoelectrons emitted by the photocathode gain kinetic energy falling through the electric field. This kinetic energy is converted into electron-hole pairs when the photoelectron impacts the diode. The generated electric pulse is read off the diode, amplified, and sent to digitizing electronics. Typical gains for the HPD are from 1000 to 2000. Figure 9 shows the internal design of a HPD.

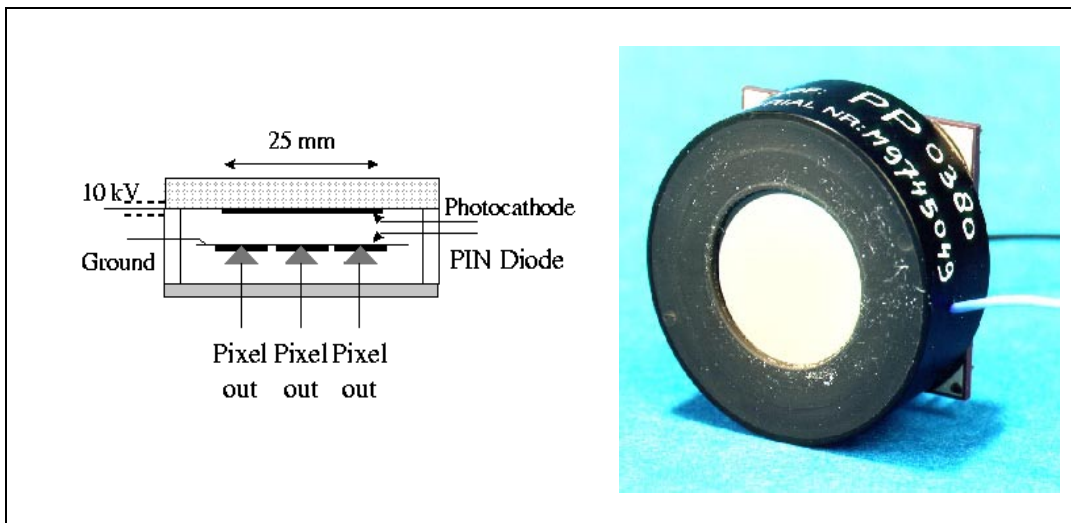


Figure 9. HPD internal structure and photograph of DEP multi-pixel HPD.

Because the low gain of the HPD requires the use of an associated amplifier, they are effectively noisier than conventional photomultiplier tubes. The estimated noise is about 1 photoelectron. A minimum ionizing signal in the calorimeter is about 10 photoelectrons, so a MIP can be clearly seen with an HPD. Figure 10 shows a test beam measurement of the muon signal through 8 layers of scintillator using an HPD for readout.<sup>9</sup>

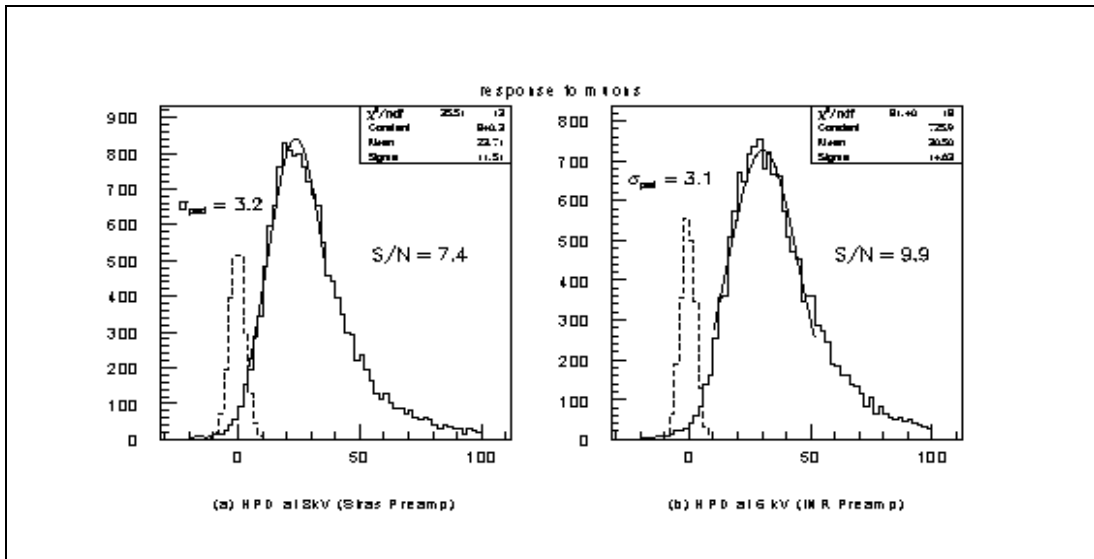


Figure 10. Test beam response for minimum ionizing tracks through the HCAL. The HPD signal is amplified and then digitized.

Because of our reliance on radioactive sources for quality control and calibration, the HPD must be able to accurately measure DC currents (supplied by the radioactive sources). The HPD has a typical leakage current of about 1 - 5 nA, with a jitter in the current of only order 10 pA. The source-induced currents are of order 5 nA, comparable to the total leakage current. Under these conditions, the HPD's have been shown to allow source current measurements of accuracy 1%.<sup>9</sup>

### Status

The HCAL barrel design has been completed. A full size barrel wedge is being fabricated in the factory and should be complete in September 1998. Another full size prototype is planned for spring 1999. The fabrication of the 36 production wedges will start in late 1999, and should be complete in late 2001. The completed wedges will be mated with the optical packages that will be built concurrently. This integration process will take place at CERN in 2000 and 2001. The wedges will be joined into half barrels in 2002, and installed into CMS in 2003.

The endcap calorimeters will be assembled in the CMS assembly hall during 2002, and installed into CMS in 2003. Electronics, trigger, and calibration systems will be integrated in 2004, in advance of detector operation in 2005.

Table 1 summarizes the properties of the CMS Hadron calorimeters.

**HCAL Summary Table**

	HB	HOB	HE	HF
$\eta$ coverage	0 - 1.3	0 - 1.1	1.3 - 3	3 - 5
$\eta$ - $\phi$ segmentation	$\sim 0.087 \times 0.087$	$\sim 0.087 \times 0.087$	$\sim 0.087 \times 0.087$	$\sim 0.175 \times 0.175$
Min. thickness				
HCAL	5.8 $\lambda$		10.3 $\lambda$	9 $\lambda$ total
+ ECAL	6.8 $\lambda$	-	11.4 $\lambda$	
+ ECAL + HO	10.5 $\lambda$		11.4 $\lambda$	
Structure	18 wedges per half-barrel 26 tonnes/wedge brass absorber 940 tonnes total	1 to 2 layers of scintillator in the barrel muon iron	monolithic endcaps 290 tonnes/end brass absorber	2 halves/end opening horizontally 98 tonnes/end brass absorber
Depth Segments (in HCAL)	H1(0.1 $\lambda$ ), H2	1	H1(0.1 $\lambda$ ), H2, $\eta < 2.5$ H2,H3, H4, $2.5 < \eta < 3$	EM (15 $X_0$ ) HAD (7.5 $\lambda$ ) Tail (2 $\lambda$ )
Sampling thickness				Fe matrix 0.3 mm quartz fibers on 2.5mm square grid
Absorber				
Scintillator	5 cm, 6 cm brass	$\sim 20$ cm iron	8 cm brass	
WLS Fiber	4 mm SCSN81 0.94mm Y11	10 mm BC408 0.94mm Y11	4 mm SCSN81 0.94mm Y11	
sampling fraction	7.5%	-	5.5%	0.85%
No. channels	5184	2160	3774	1920
No. tiles	40,000	2,500	26,000	$2 \times 10^6$ fibers
No. samples	17	1,2	20	-
Scintillator Area	2950m <sup>2</sup>	600 m <sup>2</sup>	1300 m <sup>2</sup>	3850 km fiber
PE/Sample/MIP	2pe / tile/MIP	10pe / tile/MIP	2 pe / tile/MIP	-
PE/GeV	20 pe/GeV	20pe/GeV	15pe/GeV	0.25 pe/GeV
Signal/noise for MIP	50 pe/1.5 pe (H2)	10 pe/1.5 pe	60pe/1.5 pe (H2)	0.5 pe /0.1 pe
Nominal resolution				
HCAL	90% $\oplus$ 4%	-	1.17 $\oplus$ 6.6%	200 $\oplus$ 3%
+ ECAL	112% $\oplus$ 4%			
e/h (effective)	1.3	-	1.3	2
Photodetector	HPD	HPD	HPD	PMT
gain	2000	2000	2000	$5 \times 10^4$
Max rad dose $5 \times 10^5 \text{ pb}^{-1}$ (=10 yr. operation)	0.01 Mrad	$\sim 0$	3 Mrad	100 Mrad
Dynamic range (pe) (GeV)	1pe - 70000 pe 0 - 3.5 TeV	1pe - 20000pe 0 - 1 TeV	1pe - 50000pe 0 - 3.5 TeV	1 pe - 1500 pe 0 - 7 TeV

## BIBLIOGRAPHY

1. D. Winn, et al., CMS Quartz Fiber Calorimeter, these proceedings.
2. Compact Muon Detector Technical Proposal, CERN/LHCC 94-38
3. G. Foster, J. Freeman and R. Hagstrom, Nucl. Phys. B, **A23**(1991) 93
4. J. Freeman, et al. The CDF Upgrade Calorimeter, Proc. 2nd Int. Conf on Calorimetry in HEP, Capri, Italy, 1991
5. P. de Barbaro, et al. Nucl. Instrum. Methods, **A315** (1992) 317
6. The Hadron Calorimeter Project Technical Design Report, CERN/LHCC 97-31, p25.
7. V. Barnes, CDF Endplug Calibration, these proceedings.
8. J. Freeman and W. Wu, In situ Calibration of the CMS HCAL Detector, FNAL-TM-1984
9. P. Cushman, et al., CMS HPD Development, these proceedings.